Radiographic Investigations of Micro-Ruptures in Technical Diaphrams

D. Thomsen[1)], T. Kurz [2)], R. Kaesler[2)], T.M. Buzug[1)]
[1)] Department of Mathematics and Technology, RheinAhrCampus
[2)] Integral Accumulator, Remagen

Abstract

Accumulators are used in lots of applications. So they are used as a pressure accumulator for quick energy supply to hold a constant pressure (equalization of leakage), for pulsation damping and as an element of suspension. We can differ between 3 types of accumulators: 1. Diaphragm Accumulator, 2. Piston Accumulator 3. Metal Bellow Accumulator. At applications with high requirements to permeation the diaphragm accumulators are equipped with so called multi-layer diaphragms. During test series some of these accumulators failed because of big gas losses. At a first look, no external damage could be seen, so that the damage was assumed in the internal layer.
In this contribution the results of a detailed X-ray based non-destructive testing (NDT) of accumulator membranes are reported. This includes digital X-ray fluoroscopy using a Philips Computed Radiography (PCR) system as well as conventional and micro CT investigations.

1 Introduction

Accumulators were originally developed as energy accumulators. Modern hydro-accumulators are also used for damping, to balance out leakage and volume and for pulsation damping. There are diaphragm and piston accumulators and valve units used in conjunction with diaphragm accumulators.
In extreme situations a membrane leakage has been observed in a testing environment. A first optical inspection did not show any damage of the issue. Thus, due to the multi-layer structure of the membrane an inner-structure damage is suspected to be the cause of the leakage.
The internal structure of the multi-layer diaphragms is shown in figure 1.

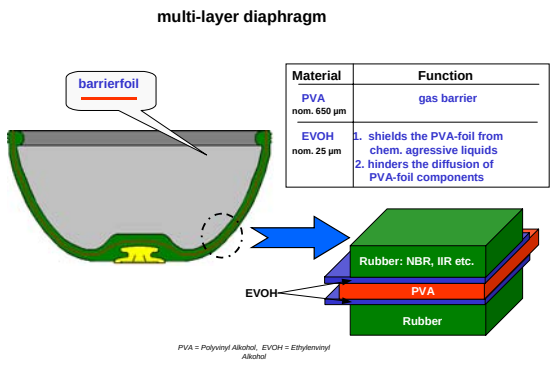

Figure 1: Overview of multi-layer diaphragm assembly.

The diaphragm used in the accumulator consists mainly of nitrile rubber (NBR) and contains an internal layer of polyvinyl alcohol (PVA) which works as a gas barrier. This layer is covered by two thin layers of ethylene vinyl alcohol copolymer (EVOH) which have to shield the PVA-foil from chemically aggressive liquids and prevent the PVA-foil components from diffusion.

2 X-ray Fluoroscopy

As a first low-cost easy to use method in the investigation of gas losses, we used a digital X-ray fluoroscopy system. In Figure 2 the setup and the data of the PCR system are shown. The data do not reveal any significant difference between a new diaphragm (upper part) and the damaged diaphragm from the test series (lower part). It shows no details about the internal structures of the component parts and especially no indication about the cause of the gas loss. The reason for this is the low contrast of X-ray fluoroscopy systems compared to CT X-ray systems.

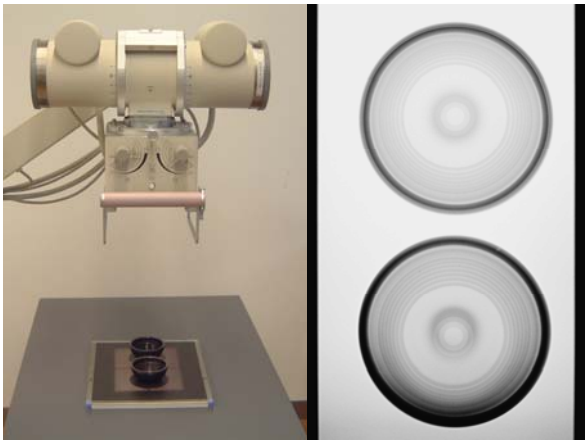

Figure 2: Setup of the X-ray fluoroscopy system with a digital cassette (resolution 2364 x 2964 pixel) and data of reference membrane (top) and membrane after test series (bottom).

3 Conventional CT

To increase contrast we used a Philips Secura CT, a conventional medical spiral CT-System. The 3-D reconstruction of the CT-data in figure 3 shows different areas of reduced absorption which can be divided into two categories:

- large detachments of the inner rubber layer mainly in the center of the diaphragm (see also figure 4 - section through the center of the membrane)
- multiple isolated lineaments located in the concentric strengthened middle part of the diaphragm. These lineaments are orientated on meridians.

With their high contrast the CT-data reveal detailed information on structural irregularities in the membrane. However, for further investigations of the lineaments presented in the dataset a higher spatial resolution is necessary.

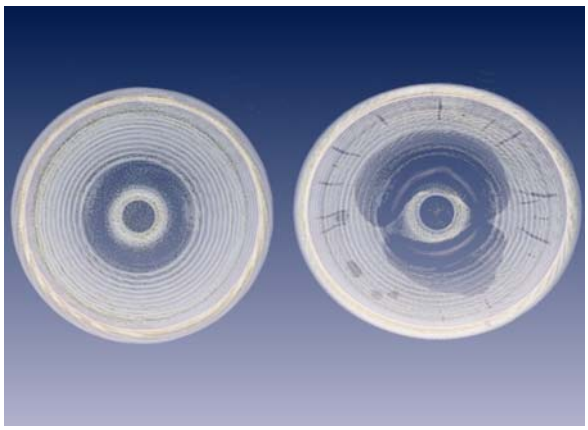

Figure 3: 3-D reconstruction of the CT data of reference membrane (left) and membrane after test series (right).

Figure 4: Section from the center of the membrane**.**

4 Micro CT

4.1 Spatial Resolution

To combine high contrast and high spatial resolution a micro CT was used.
The relevant components of such CT systems are micro focus X-ray tube and a high resolution 2D-CCD detector array. The spatial resolution is limited by the size of the focus (see figure 5) and the size of the detector elements.

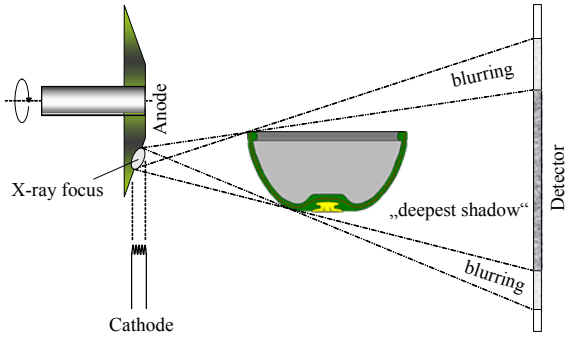

Figure 5: The inclination of the anode controls the optical size of the X-Ray focus. A larger X-ray focus increases the blurring of the image.

The so called modulation-transfer function *MTF* gives the resolution for spectral frequencies q in line pairs per millimetre [1]:

$$MTF_{system}(q) = MTF_{focus}(q)\,MTF_{detector}(q) = \left|\frac{\sin(\pi b_F q)}{\pi b_F q}\right| \left|\frac{\sin(\pi b_D q)}{\pi b_D q}\right|$$

Typical focus sizes are b_f = 1 mm for conventional medical CTs and b_f < 10 µm for micro CTs.
Figure 6 shows the characteristics of the *MTF* of a conventional medical CT and a micro CT, respectively.

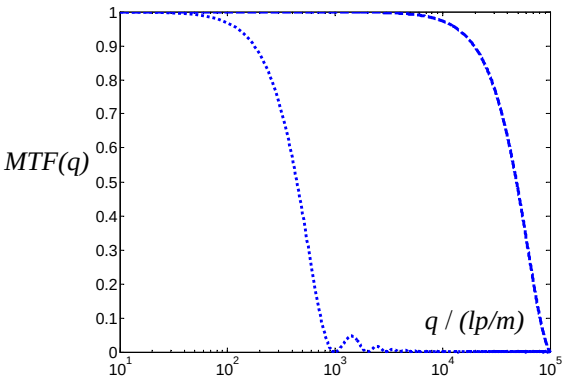

Figure 6: Frequency dependent modulation-transfer-function of conventional CT (doted curve) and micro-CT (dashed curve).

As a consequence of the small focus size of micro CTs the anode current is limited to $I < 100$ µA. This affects the intensity of the X-ray spectrum and limits the range of possible probe materials.
The micro CT by the Belgian company SkyScan shown in figure 7 uses a 12 Bit CCD-Chip with a pixel matrix of 1024 x 1024 and a pixel size of about 10 µm which is coupled via fibre optics to a scintillation crystal. In conventional CTs the detector dimension b_d is typically found in the order of 1 mm.
SkyScan gives a specification of spatial resolution of 10 µm for the 1072 scanner used in the experiments shown here [2,3,4].

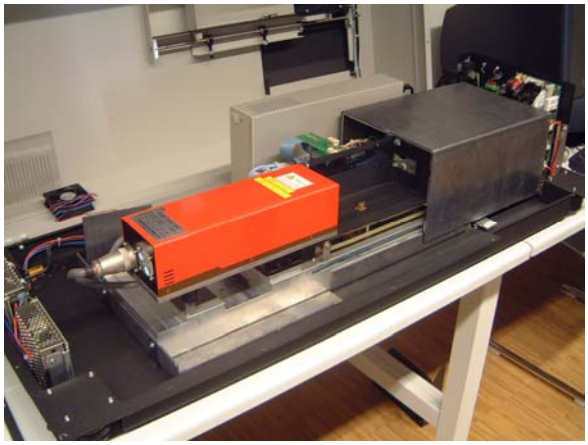

Figure 7: Setup of micro-CT.

4.2 Imaging Results

Figure 7 displays the setup of the micro CT which can be used to investigate objects up to a size of 2 cm^3.
The 3-D reconstruction of the micro CT data of one of the lineaments shown in figure 9 reveals that there are ruptures especially in the covering EVOH layers.

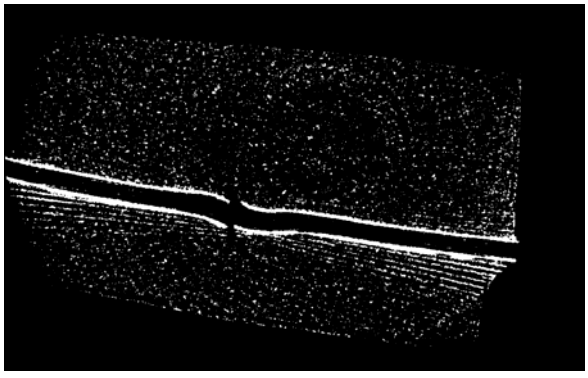

Figure 8: Single tomographic section of the membrane rupture.

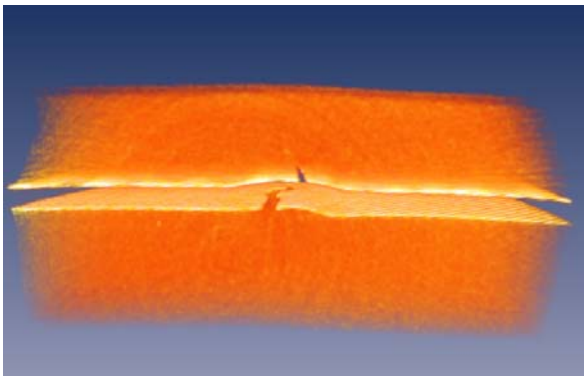

Figure 9: 3-D reconstruction of the membrane rupture.

5 Microscopic Evaluation

The microscope pictures in figure 10 show a part of the inner EVOH-layer in different enlargements. The higher magnification in figure 10b clearly indicates that the material becomes brittle and fragile along the fold structures.

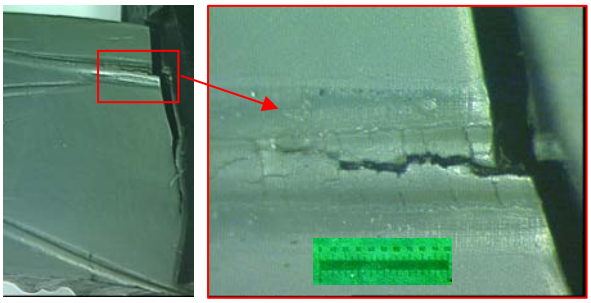

Figure 10: Microscope picture of the fold structure (width approx. 1 mm).

6 Resume

The production of the membranes apparently leads to folds in the internal EVOH/PVA-layer. The cause of gas losses are ruptures in these folds.

References

[1] T. M. Buzug, *Einführung in die Computertomographie*, Springer-Verlag, Heidelberg, 2004.
[2] A. Sassov 1999, *Desktop X-ray Micro-CT*, in: Proc. of the DGZiP BB67-CD, Computerized Tomography for Industrial Applications and Image Processing in Radiology (Berlin) 165.
[3] A. Sassov 2002, *Desktop X-ray Micro-CT Instruments*, Proc. of SPIE **4503**, 282.
[4] A. Sassov 2002, *Comparison of Fan-Beam, Cone-Beam and Spiral Scan Reconstruction in X-Ray Micro-CT*, Proc. of SPIE **4503**, 124.